

## Effects of tissue absorption on calculation of mean photon path length using modified Beer-Lambert law

SHANG Yu<sup>1,2</sup>, GUI Zhi-guo<sup>1,2</sup>

(1. *Science and Technology on Electronic Test & Measurement Laboratory, North University of China, Taiyuan 030051, China;*

2. *Key Laboratory of Instrumentation Science & Dynamic Measurement (North University of China), Ministry of Education, Taiyuan 030051, China)*

**Abstract:** The mean path length (MPL) of photons is a critical parameter to calculate tissue absorption coefficient as well as blood oxygenation using modified Beer-Lambert law, where in the differential path factor (DPF) is often assumed as constant over range of tissue absorption. By utilizing the Monte Carlo (MC) simulation of photon migrations in the leg, this study used four approaches to estimate MPL, and compared them with that determined by the MPL definition. The simulation results indicate that the DPF is remarkably affected by tissue absorption, at approximate 10% variation. A linear model is suggested to calculate MPL for measurements of tissue absorption as well as blood oxygenation using modified Beer-Lambert law.

**Key words:** mean path length (MPL); photon Monte Carlo (MC) simulation; modified Beer-Lambert law; tissue absorption

**CLD number:** O433.1

**Document code:** A

**Article ID:** 1674-8042(2016)02-0110-05

**doi:** 10.3969/j.issn.1674-8042.2016.02.003

## 0 Introduction

Beer-Lambert law is a commonly used algorithm to calculate the concentration of a substance in liquid solution or gas by using a variety of physical particles, such as X-ray,  $\gamma$  ray, and more often, near-infrared (NIR) light. This law is mathematically expressed as below<sup>[1-7]</sup>

$$\ln(I_s/I_d) = \mu_a d, \quad (1)$$

where  $I_s$  and  $I_d$  are the doses of physical particles injected from the source and collected by the detector, respectively,  $\mu_a$  is absorption coefficient of the substance to be measured, and  $d$  is the distance between the source and detector.

Eq. (1) indicates that all detected physical particles travel in a straight way and their directions are never altered before arriving at the detector. In other words, the path length of the particles is equal to the

separation ( $d$ ) of source and detector that are placed on both sides of substance solution.

The assumption of particles with straight path way meets many measurements on thin substance samples using spectrometer. It is also approximately accurate for hard particles such as X-ray and  $\gamma$  ray, whose directions are seldom altered even if penetrating through bulk and thick samples.

Beer-Lambert law, however, is no longer valid when using light, especially in NIR range, to detect the biological tissue in vivo. The primary reason is that there are various scatterers within tissues, such as organelles, mitochondria, as well as red blood cells (RBCs). Due to scatterers, the photons (i. e. light particles) frequently change direction before arriving at the detector. As a results, the path lengths of photons are remarkably increased. To account for the scattering events (i. e. photon path direction changes due to the scatterers), Eq. (1) is modified

**Received date:** 2015-03-22

**Foundation items:** Research Funds from North University of China (No. 130087).

**Corresponding author:** SHANG Yu (yushang@nuc.edu.cn)

as<sup>[8-14]</sup>

$$\ln(I_s/I_d) = \mu_a L. \quad (2)$$

Eq. (2) is called “modified Beer-Lambert law”. Here  $I_s$  and  $I_d$  denote the light intensity (i. e. photon amount) at source and detectors, respectively,  $L$  is the mean path length (MPL). Compared with Eq. (1), it is clear that source-detector (S-D) separation ( $d$ ) is replaced by MPL ( $L$ ). Accordingly, a parameter, called “differential path factor (DPF)”, is defined as  $DPF=L/d$ .

Eq. (2) is more often used in diffuse optical spectroscopy (NIRS) to measure the blood oxygenation in the tissue. This concept was also extended to measure the blood flow change in the tissue<sup>[15]</sup>. Here the term “diffuse” denotes the light diffusion caused by scattering events. Eq. (2) takes both factors of absorption and scattering into consideration, and utilizes multiple wavelengths of light to separate the oxy-hemoglobin and deoxy-hemoglobin, two major absorbers in the tissue blood. More oxygenation parameters, such as total hemoglobin concentration and oxygen saturation, can be calculated from oxy-hemoglobin and deoxy-hemoglobin.

Although there are some partial differential equations to depict the light diffusion due to absorption and scattering, modified Beer-Lambert law is widely adopted to calculate the oxygenation changes, owing to simple instrument requirement and fast computations.

When using Eq. (2) to calculate absorption coefficient ( $\mu_a$ ),  $L$  must be a known parameter, which is, in practice, assumed to be proportional to  $d$ . Accordingly, DPF is assumed to be constant regardless  $\mu_a$  variation. Under this assumption, the unknown  $\mu_a$  can be calculated with Eq. (2) as long as light intensity and S-D separation ( $d$ ) are measurable.

The DPF and the corresponding MPL, however, are not easily determined through experiments<sup>[16]</sup>. Because of light diffusion, the photons injected from the same source have different path lengths. There is no unique method to estimate the MPL through the path lengths of all detected photons. In this study, a total of four approaches, in different ways to estimate the MPL from individual detected photons,

were compared. In contrast to the conventional method that measures the photon path length through the experiments, a Monte Carlo (MC) simulation of photon migration within the tissue was utilized to determine the path lengths of each packet of detected photons. The algebra and geometrical averaging methods were adopted, respectively, to calculate the MPL, and compared with those determined by the definition of modified Beer-Lambert law.

## 1 Methods

### 1.1 Approaches to estimate MPL of photons

Approach 1 is the MPL calculated directly from modified Beer-Lambert law, i. e.

$$L_{\text{mean},1} = \ln(I_s/I_d)/\mu_a. \quad (3)$$

As seen from Eq. (3), approach 1 is determined by the light intensity (i. e. the sum of the photons at source and the detector), not a derivative of individual photon path lengths. Here we selected it as a standard to evaluate other approaches.

Although the approach of modified Beer-Lambert law is well recognized and the MPL can be determined through the experiments, there is a lack of appropriate approaches to directly estimate the MPL from individual photon path length. Thus, we established approaches 2–4 in this study by averaging over the path lengths from individual photons in different ways, specified as below.

The direct average of the photon path length over detected photon packet is selected as approach 2. Here the photons in each packet from the source are assumed to have an identical trajectory within the tissue. Assuming a total of  $n$  photon packets are detected, approach 2 can be depicted by

$$L_{\text{mean},2} = \frac{1}{n} \sum_{i=1}^n L_i, \quad (4)$$

where  $L_i$  is the path length of  $i$ -th photon packet. Notice that only the weight factor from the source is considered in Eq. (4). In other words, each photon packet from the source is treated to be equal. The weight factor from the detector is ignored.

By contrast, the weighted average of path length

over detected photon packet is selected as approach 3, which is depicted by

$$L_{\text{mean},3} = \sum_{i=1}^n \omega_i L_i, \quad (5)$$

where  $\omega_i$  is the weight factor in the detector, quantifying how many percentage of photons are collected in  $i$ -th detected photon packet. A 100% is defined as the total percentage of all detected photon number. According to the definition, we have

$$\sum_{i=1}^n \omega_i = 1. \quad (6)$$

Notice that the weight factor from the detector is considered in Eq. (6). In other word, each detected photon is treated to be equal. The weight factor from the source (i. e. photon packet) is ignored.

The arithmetic average of MPL from approaches 2 and 3 is selected as approach 4, i. e.

$$L_{\text{mean},4} = (L_{\text{mean},2} + L_{\text{mean},3})/2. \quad (7)$$

The geometric average of MPL from approaches 2 and 3 is selected as approach 5, i. e.

$$L_{\text{mean},5} = \sqrt{L_{\text{mean},2} \cdot L_{\text{mean},3}}. \quad (8)$$

Approaches 4 and 5 are two ways to balance between approach 2 (considering the weight of source) and approach 3 (considering the weight of detector).

## 1.2 Monte Carlo simulation of photons

A free software Monte carlo modeling of photon migration in voxelized media (MCVM), developed in the university laboratory<sup>[17]</sup> was adopted to perform the MC simulations of photon migrations in the tissue. The MCVM enables simulation of photon migrations in highly scattered media, for which the media was divided into a large number of voxels. A cylinder with diameter of 10 cm and length of 20 cm as shown in Fig. 1, was adopted to mimic the human leg. For the simulation setup, the cylinder was divided into 2 million ( $100 \times 100 \times 200$ ) voxels, with size of  $1 \text{ mm}^3$  for each voxel. The source (S) and detector (D) was placed on the middle part of cylinder surface. The S-D separation was fixed at 2.0 cm. To investigate the influence of tissue absorption,  $\mu_a$  was centered at  $0.1 \text{ cm}^{-1}$  and varied in range from 0.06

to  $0.14 \text{ cm}^{-1}$ , with step interval of  $0.02 \text{ cm}^{-1}$ . For each  $\mu_a$  value, 10 million photon packets were launched from the source and injected into the tissue. Each photon was either absorbed or scattered by the tissue, and determined by the probability relevant to the absorption ( $\mu_a$ ) or scattering ( $\mu'_s$ ) coefficients. The photons following multiple scattering events and escaping at the given location were collected by the detector.

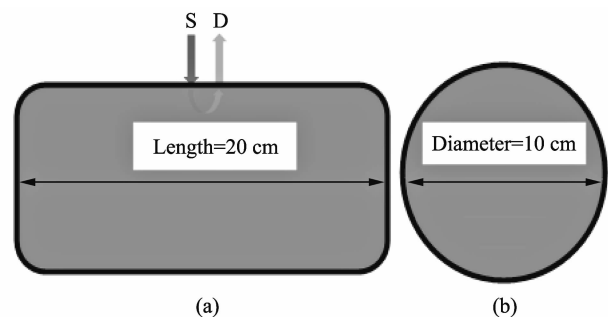


Fig. 1 Schematic diagram of cylinder

## 1.3 Data analysis

For each  $\mu_a$  value, path length ( $L_i$ ) and weight ( $\omega_i$ ) of each photon packet were determined by MC simulation, and the MPL and DPF were calculated by using approaches 1 – 5, as specified in Eqs. (3) – (8). Correlation and linear regression methods were adopted to exam the relationship between  $\mu_a$  value and MPL. A variation coefficient, i. e.  $cv = 100\% \cdot \text{Std}(\text{DPF})/\overline{\text{DPF}}$ , was used to quantify the DPF variability when  $\mu_a$  changes. Here  $\text{Std}(\text{DPF})$  and  $\overline{\text{DPF}}$  denote the standard derivation and mean value of DPF, respectively. Additionally, the square of correlation coefficient ( $R^2$ ) and  $p$ -value were used to evaluate the linear relationship between  $\mu_a$  and MPL.

## 2 Results

When approach 1 was used, the MPL and DPF in 5 steps of  $\mu_a$  variation are shown in Fig. 2(a). An excellent relationship between MPL and  $\mu_a$  values is found ( $R^2 = 0.99$ ,  $p < 0.0001$ ), as denoted by

$$y = a_0 + a_1 x, \quad (9)$$

where the intercept and slope for the linear relationship are represented by  $a_0$  and  $a_1$ , respectively. Ideally, the intercept should be zero if DPF is constant.

However, a non-zero intercept (i. e.  $a_0 = 22.0$ ) was found. Furthermore, the DPF value in each step of  $\mu_a$  value is shown in Fig. 2(b), which exhibits the remarkable variation in DPF caused by the non-zero intercept.

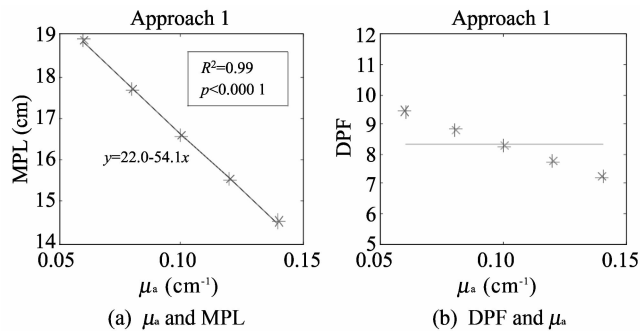


Fig. 2 Correlation analysis and linear regression

When  $\mu_a$  changes, the intercepts and slopes of MPL calculated through approaches 1–5, as well as

the mean ( $m$ ) and variation coefficient ( $cv$ ) of DPF are summarized in Table 1. All approaches lead to positive intercepts, and reach maximal and minimal values when approach 2 and 3 were used, respectively. The largest (11.7%) and smallest (7.9%) variations of DPF were found in approach 3 and 2, respectively. The approach 5 is closest to approach 1 in most calculated parameters. In fact, both arithmetic average (approach 4) and geometric average (approach 5) account for the balance between the source and detector, overcoming the limitations of direct average and weighted approaches (approach 2 and approach 3). Moreover, the geometric average approach (approach 5) minimizes the effects of extreme large and extreme small values in the data, thus the result is closest to the mean value calculated by the MPL definition.

Table 1 MPL and DPF in 5 steps of  $\mu_a$  variations

Variable	Parameter	Approach 1	Approach 2	Approach 3	Approach 4	Approach 5
MPL	$a_0$	22.0	30.5	16.9	26.3	25.9
	$a_1$	-54.1	-60.7	-45.3	-57.4	-57.8
DPF	$m$	8.3	12.2	6.2	10.3	10.1
	$cv(\%)$	10.3	7.9	11.7	8.9	9.1

### 3 Conclusion

The results indicate that the MPL decreases linearly with the increase of  $\mu_a$  value. Any approach, however, leads to a non-zero intercept. As the results, DPF varies around 10% over the steps of  $\mu_a$  values. Of all adopted approaches, approach 5 is closest to approach 1, and representative of the true MPL and DPF.

In summary, this study shows that the MPL generated by combination of the photon path averages (i. e. approach 5) is closest to the true value. The DPF is remarkably affected by  $\mu_a$  value. Thus, a linear model with non-zero intercept, rather than DPF, is suggested to calculate MPL, for measurements of tissue absorption as well as blood oxygenation using Beer-Lambert law.

### References

- [1] Swinehart D F. The Beer-Lambert Law. Journal of Chemical Education, 1962, 39(7): 333-335.
- [2] Ricci R W, Ditzler M, Nestor L P. Discovering the Beer-Lambert Law. Journal of Chemical Education, 1994, 71 (11): 983-985.
- [3] Zardecki A, Tam W G. Multiple scattering corrections to the Beer-Lambert law. 2; Detector with a variable field of view. Applied Optics, 1982, 21(13): 2413-2420.
- [4] Jodpimai S, Boonduang S, Limsuwan P. Inline ozone concentration measurement by a visible absorption method at wavelength 605 nm. Sensors and Actuators B-Chemical, 2016, 222(8): 8-14.
- [5] Marcus T C E, Ibrahim M H, Ngajikin N H, et al. Optical path length and absorption cross section optimization for high sensitivity ozone concentration measurement. Sensors and Actuators B-Chemical, 2015, 221: 570-575.
- [6] Chen C, Florian K, Rajesh K, et al. Recovering the superficial microvascular pattern via diffuse reflection imaging: phantom validation. Biomedical Engineering Online, 2015, 14(1): 87.
- [7] Abay T Y, Kyriacou P A. Reflectance photoplethysmography as noninvasive monitoring of tissue blood perfusion. IEEE Transactions on Biomedical Engineering, 2015, 62 (9): 2187-2195.
- [8] Huang A, Ngu X. The application of extended modified Lambert Beer model for measurement of blood carboxyhemoglobin and oxyhemoglobin saturation. Journal of Inno-

- vative Optical Health Sciences, 2014, 7(3): 1450026
- [9] Talukdar T, Moore J H, Diamond S G. Continuous correction of differential path length factor in near-infrared spectroscopy. *Journal of Biomedical Optics*, 2013, 18(5): 056001.
- [10] Strangman G, Franceschini M A, Boas D A. Factors affecting the accuracy of near-infrared spectroscopy concentration calculations for focal changes in oxygenation parameters. *Neuroimage*, 2003, 18(4): 865-879.
- [11] Yoshitani K, Kawaguchi M, Miura N. Effects of hemoglobin concentration, skull thickness, and the area of the cerebrospinal fluid layer on near-infrared spectroscopy measurements. *Anesthesiology*, 2007, 106(3): 458-462.
- [12] Mei L, Somesfalean G, Svanberg S. Pathlength determination for gas in scattering media absorption spectroscopy. *Sensors*, 2014, 14(3): 3871-3890.
- [13] Maikala R V. Modified Beer's Law-historical perspectives and relevance in near-infrared monitoring of optical properties of human tissue. *International Journal of Industrial Ergonomics*, 2010, 40(2): 125-134
- [14] Gobrecht A, Bendoula R, Roger J M, et al. A new optical method coupling light polarization and Vis-NIR spectroscopy to improve the measurement of soil carbon content. *Soil & Tillage Research*, 2016, 155: 461-470.
- [15] Baker W B, Parthasarathy A B, Busch D R, et al. Modified Beer-Lambert law for blood flow. *Biomedical Optics Express*, 2014, 5(11): 4053-4075.
- [16] Duncan A, Meek J H, Clemence M, et al. Optical path-length measurements on adult head, calf and forearm and the head of the newborn infant using phase resolved optical spectroscopy. *Physics in Medicine and Biology*, 1995, 40(2): 295-304 .
- [17] LI Ting, GONG Hui, LUO Qing-ming. MCVM: Monte Carlo modeling of photon migration in voxelized media. *Journal of Innovative Optical Health Sciences*, 2010, 3(2): 91-102.

## 利用修改的比尔-郎伯定律计算组织吸收 对光子平均路径长度的影响

尚 禹<sup>1,2</sup>, 桂志国<sup>1,2</sup>

(1. 中北大学 电子测试技术重点实验室, 山西 太原 030051;

2. 中北大学 仪器科学与动态测试教育部重点实验室, 山西 太原 030051)

**摘要:** 在使用修改的比尔-郎伯定律计算组织的吸收系数以及血氧含量时, 平均路径长度(MPL)是一个重要的参数, 由此参数可得到微分路径因子(DPF), 而 DPF 通常假定为在一定组织吸收范围内是一个常数。通过腿部的光子蒙特卡罗仿真, 本论文使用四种方法来估计 MPL, 并与 MPL 的原始定义进行对比。仿真结果表明, DPF 显著受到组织吸收的影响, 表现为 10% 的数值变化。因此, 使用线性模型将比使用修改的比尔-郎伯定律能更好地计算组织的吸收系数以及血氧含量。

**关键词:** 平均路径长度(MPL); 光子蒙特卡罗仿真; 修改的比尔-郎伯定律; 组织吸收

**引用格式:** SHANG Yu, GUI Zhi-guo. Effects of tissue absorption on calculation of mean photon path length using modified Beer-Lambert law. *Journal of Measurement Science and Instrumentation*, 2016, 7(2): 110-114. [doi: 10.3969/j.issn.1674-8042.2016.02.003]